

APPENDIX

Targeted delivery of a phosphoinositide 3-kinase γ inhibitor to restore organ function in sepsis through dye-functionalized lipid nanocarriers

Authors Adrian T. Press^{1,2,3}, Petra Babic^{1,3}, Bianca Hoffmann⁴, Tina Müller^{1,3}, Wanling Foo¹, Walter Hauswald⁵, Jovana Benecke^{1,3}, Martina Beretta^{1,3}, Zoltán Cseresnyés⁴, Stephanie Hoepfener^{6,7}, Ivo Nischang^{6,7}, Sina M. Coldewey^{1,3,8}, Markus H. Gräler^{1,3}, Reinhard Bauer¹⁰, Falk Gonnert^{1,3}, Nikolaus Gaßler⁹, Reinhard Wetzker^{1,3}, Marc Thilo Figge^{2,4,11}, Ulrich S. Schubert^{3,6,7}, Michael Bauer^{1,3,6}

Affiliations

¹ Department of Anesthesiology and Intensive Care Medicine, Jena University Hospital, Am Klinikum 1, 07747 Jena, Germany

² Medical Faculty, Friedrich Schiller University Jena, Bachstr. 18, Jena, Germany

³ Center for Sepsis Control and Care, Jena University Hospital, Am Klinikum 1, 07747 Jena, Germany

⁴ Research Group Applied Systems Biology, Leibniz Institute for Natural Product Research and Infection Biology - Hans Knoell Institute, Jena, Germany

⁵ Leibniz Institute of Photonic Technology, Albert-Einstein-Straße 9, 07745 Jena, Germany

⁶ Jena Center for Soft Matter (JCSM), Friedrich Schiller University Jena, Philosophenweg 7, 07743 Jena, Germany

⁷ Laboratory of Organic and Macromolecular Chemistry (IOMC), Friedrich Schiller University Jena, Humboldtstrasse 10, 07743 Jena, Germany

⁸ Septomics Research Centre, Jena University Hospital, Jena, Germany

⁹ Institute of Molecular Cell Biology, Jena University Hospital, Jena, Germany

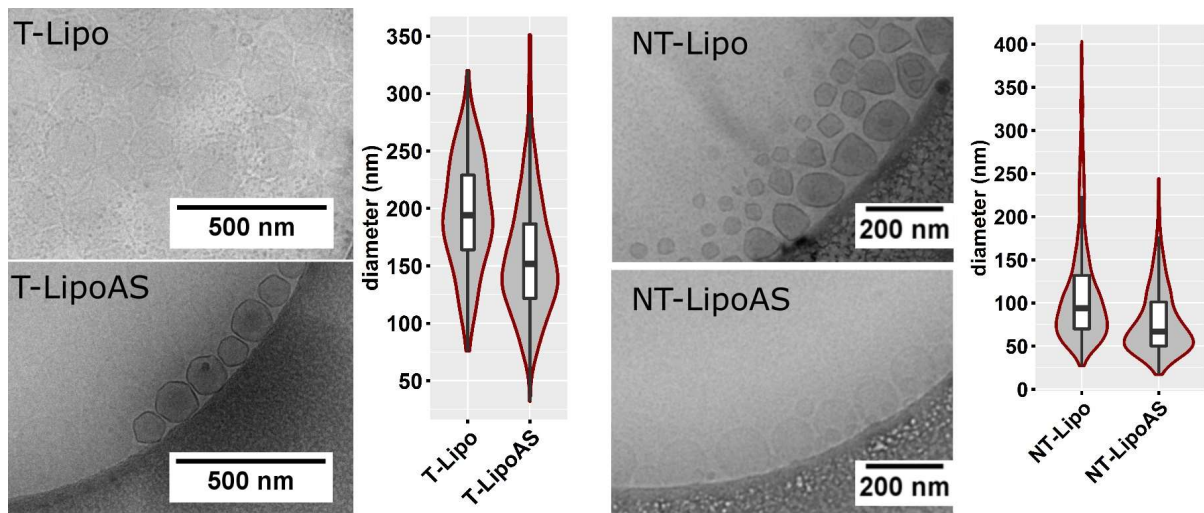
¹⁰ Section of Pathology, Institute of Forensic Medicine, Jena University Hospital, Am Klinikum 1, 07747 Jena, Germany

¹¹ Institute of Microbiology, Faculty of Biological Sciences, Friedrich Schiller University, Jena, Germany

Correspondence to michael.bauer@med.uni-jena.de

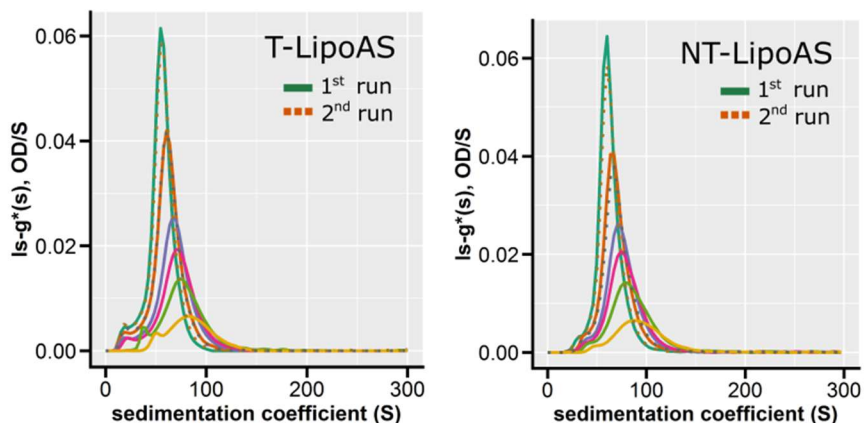
Table of Content

Appendix Figure S 1: Cryo-Transmission electron microscopy with size quantification of non-targeted Liposomal formulation.	3
Appendix Figure S2: Analytical ultracentrifugation of AS605240 loaded liposomes.....	4
Appendix Figure S3: Effects of targeted AS605240 delivery on the inflammatory response.	5
Appendix Figure S4: Scheme on processing and analysis of multispectral optoacoustic tomography (MSOT) images for the quantification of liver function by indocyanine green (ICG) clearance.	6
Appendix Figure S5: Effects of the non-targeted liposomal AS605240 formulation on survival in the peritoneal contamination and infection (PCI) sepsis model.	7
Appendix Table S1: PI3Ky expression in human tissue biopsies.	9
Appendix Table S2: Characterization of primary human hepatocyte donor pools (Lonza, Switzerland).....	10
Appendix Table S3: p-Value Tables for Figures 2 to 5 in the main manuscript and Appendix Figure S3 and S5.....	11



Appendix Figure S 1: Cryo-Transmission electron microscopy with size quantification of non-targeted Liposomal formulation.

Diameter as measured from **TEM images** (ImageJ). Median box-plot with 0.25;0.75 IQR; whiskers 0.95 percentile, violin-plots depict density. NT-Lipo 14 images = 847 liposomes, NT-LipoAS 15 images = 540 liposomes, T-Lipo 5 images = 184 liposomes, T-LipoAS 12 images = 503 liposomes

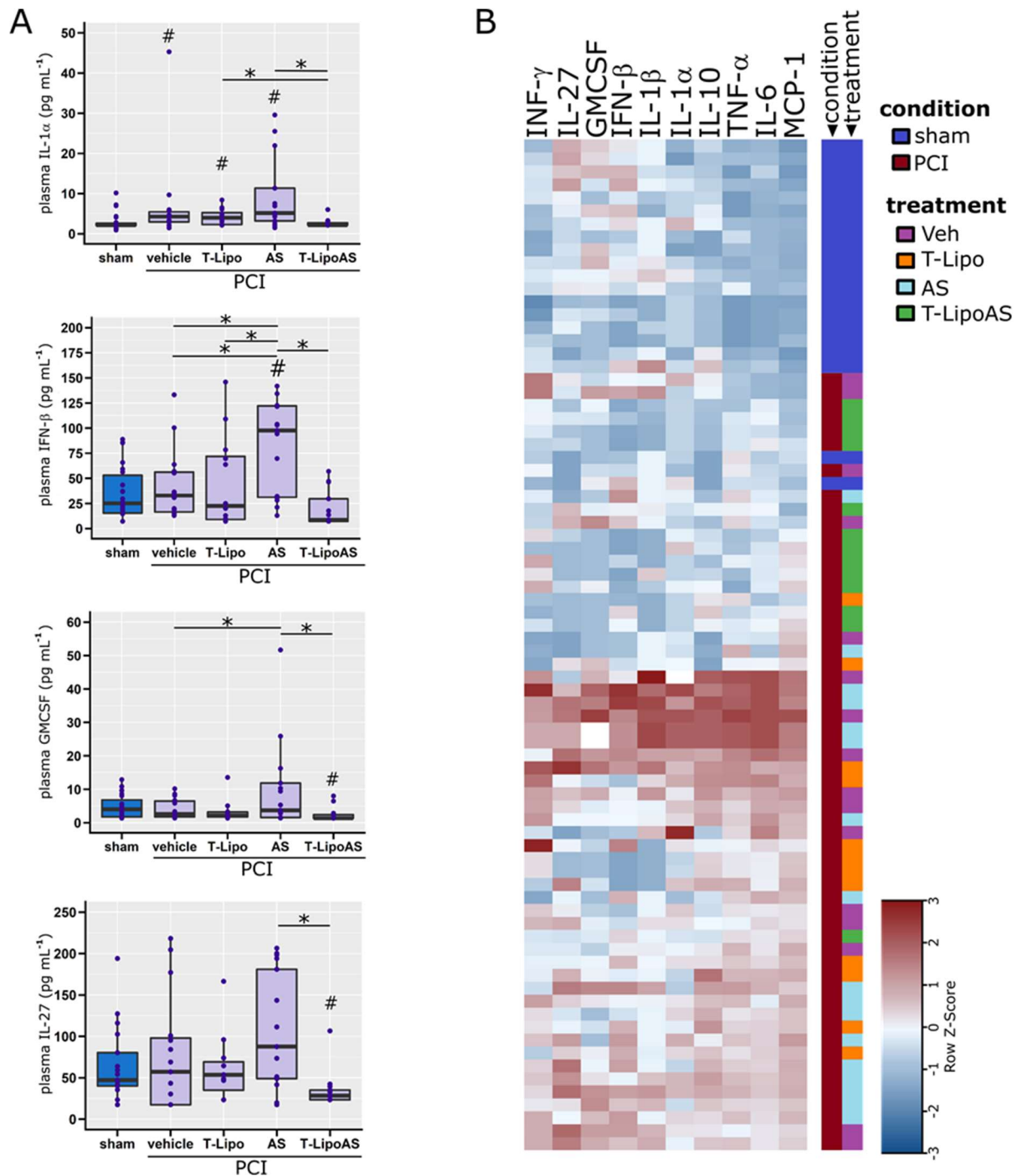


Appendix Figure S2: Analytical ultracentrifugation of AS605240 loaded liposomes.

Analytical ultracentrifugation was performed with different concentrations of liposomes. The optical density monitored the sedimentation at 496 nm. Data analysis was accomplished with the $ls - g^*(s)$ model in Sedfit (version 15.01b). The $ls - g^*(s)$ model represents a least-squares boundary analysis under the assumption of non-diffusing species and resolves the apparent differential distribution of sedimentation coefficients.

The decrease of liposomal concentration shifted the sedimentation coefficient distributions toward larger values (solid lines). Finally, sedimented liposomes were resuspended by shaking the ultracentrifuge cells, then another sedimentation velocity analysis (dotted lines). Again, very similar results were observed at all concentrations, indicating the stability of liposomes during sedimentation and after resuspension leading to the observation of identical populations.

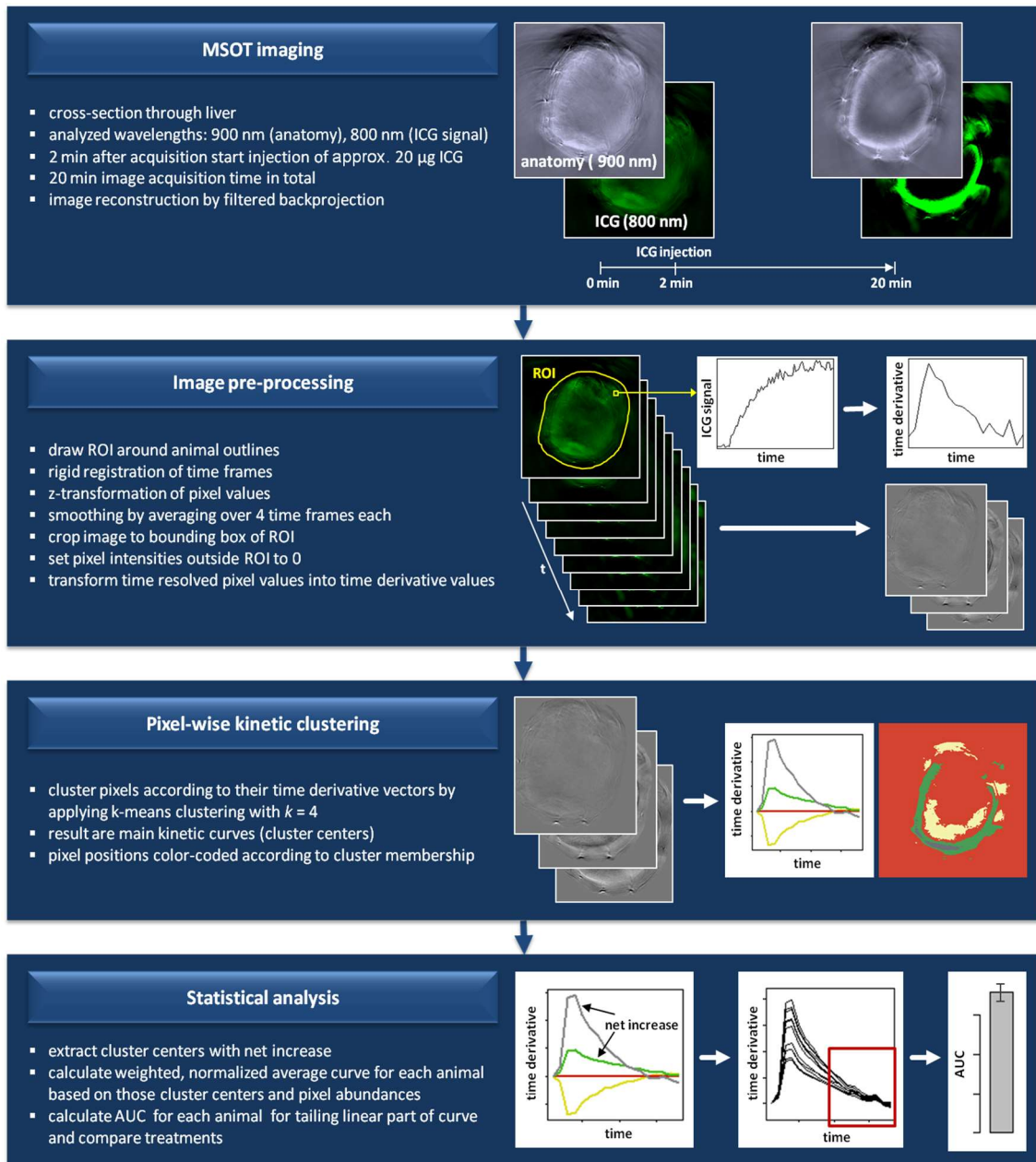
Each liposomal formulation was analyzed at six different concentrations. The spun down liposomes were resuspended by shaking the cells and re-analyzed, leading to an identical result, indicating stability. Experiments were performed for six different liposome concentrations per formulation in one replicate for each liposomal formulation.



Appendix Figure S3: Effects of targeted AS605240 delivery on the inflammatory response.

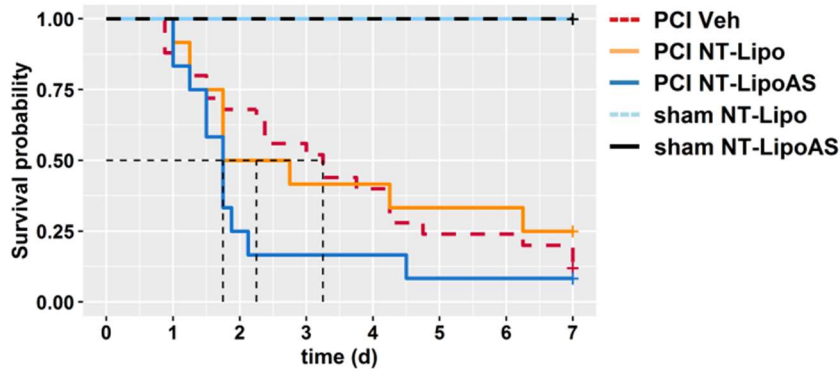
(A) Pro-inflammatory-cytokines essential for the host defence were analyzed in EDTA-plasma from PCI and sham animals. # $p < 0.05$ against sham, * $p < 0.05$ as indicated; Kruskal-Wallis ANOVA with controlled false-discovery rates (Benjamini-Hochberg procedure). The p-values are given in Appendix Table S3.

(B) Cytokine profiles are depicted in a self-organizing heat-map according to their similarity of appearance in plasma. Information on replicates can be found in Figures 3 B and 3 C).



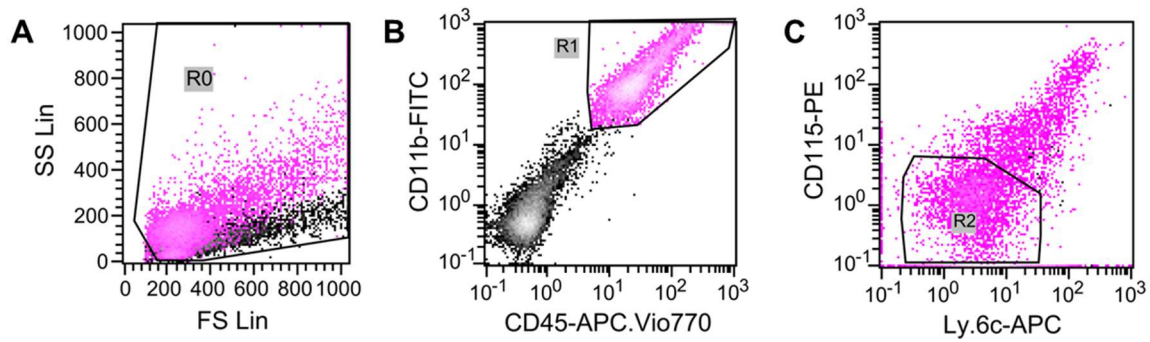
Appendix Figure S4: Scheme on processing and analysis of multispectral optoacoustic tomography (MSOT) images for the quantification of liver function by indocyanine green (ICG) clearance.

MSOT imaging is performed to derive time-resolved cross-sectional images of liver tissue and ICG distribution. MSOT image stacks are first pre-processed to normalize ICG intensity values and smooth time course data. The time derivatives of pixel intensities within a region of interest (ROI) from one-time frame to the next serve as input for pixel-wise kinetic clustering. By applying k-means clustering with k set to 4, 4 main kinetic curves (cluster centers) present in the ROI are extracted, and color-coded images are generated to visualize the spatial distribution of those clusters for each animal. For quantification of ICG signal, only those cluster centers reflecting signal net increase are taken into account and combined into one curve, incorporating the respective abundances of pixels for each animal individually. All known three phases of ICG pharmacokinetics are clearly evident in those curves: first-pass (peak), re-distribution (exponential decay) and the final linear phase representing the dye-clearance through the liver. The area under the curve (AUC) was calculated from the linear decay phase to estimate the elimination capacity of the liver.



Appendix Figure S5: Effects of the non-targeted liposomal AS605240 formulation on survival in the peritoneal contamination and infection (PCI) sepsis model.

Group sizes for sham groups NT-Lipo: 6 (50% female), NT-LipoAS: 2 (50% female) animals. For PCI (sepsis) groups: Veh: 25 (56% female), NT-Lipo: 12 (50% female), NT-LipoAS: 12 (50% female) animals. The survival is monitored for seven days in this model. In the first two or three days, the acute phase had passed and increasingly processes related to a cornification occur. Animals appear phenotypically healthy after five to seven days. However, it is common in this model for abscesses to occur without visible symptoms, which in some cases may even be macroscopically detected as early as 24 h post-infection, due to the lack of a surgical intervention cleaning and disinfecting the primary site of infection (here: abdominal cavity). These abscesses may grow and eventually rupture, causing spontaneous death unrelated to the actual experiment. As a consequence, the survival is limited here to seven days. The p-values of the statistical analysis are provided in Appendix Table S3.



Appendix Figure S6: Gating of Lavage cells for analysis.

Gating was performed as previously described by Watson et al. (J Immunol. 2016, 194(6): 2796-2809, PMID: 25681345). Peritoneal lavage and subsequent processing and staining were carried out as described in the method section. The figure depicts the gating strategy. A stained (pink) and unstained (black/grey) sample is overlaid in the XY-Plots: (A) Forward scatter vs side scatter plot with gate R0 to separate cell events from debris. (B) Fluorescence labeled double-positive CD11b+ CD45+ cells are then gated (R1) from R0. (C) CD115- and Ly-6c negative fraction of R1 is depicted, and R2 gate is used to count cells neutrophils. CD115+, Ly6c+ cells (#R1-#R2, with # stands for the number of cells in each gate) are classified as monocytes. Data are normalized to the volume used for measurement, obtaining the concentration of cells per volume lavage.

Appendix Table S1: PI3K γ expression in human tissue biopsies.

LSECs: liver sinusoidal endothelial cells, KCs: Kupffer cells (local macrophages)

Sample information		N	PI3K γ expression			
Diagnosis	Gender		Hepatocytes	LSECs, KCs	Infiltrating immune cells	endothelial cells of larger vasculature
Non-alcoholic fatty liver disease (NASH)	female	3	yes	no	Yes	yes
	male	1				
Autoimmune hepatitis (AIH)	male	1	yes	no	Yes	yes
	female	1				
Liver cirrhosis	female	2	yes	no	Yes	yes
	male	1				

Appendix Table S2: Characterization of primary human hepatocyte donor pools (Lonza, Switzerland).

Parameter	huHEP ♂ _{DP20}	huHEP ♀ _{DP20}
Number of Donors	20	20
Donor Age Average	36.9	41.1
Donor BMI Average ^a	26.3	29.2
Male Donors	100.0%	0.0%
Female Donors	0.0%	100.0%
Asian Donors	5.0%	0.0%
Afro American Donors	5.0%	10.0%
Caucasian Donors	80%	85.0%
Other Donors	10.0%	5.0%
No Drugs/ Alcohol/ Tobacco	45.0%	60.0%
Illicit Drug use	35.0%	20.0%
Tobacco Use	35.0%	20.0%
Heavy alcohol use ^b	5.0%	5.0%
Serologies CMV	Positive	Positive
Serologies EBV	Positive	Positive
Serologies HBV	Negative	Negative
Serologies HCV	Negative	Negative
Serologies HIV	Negative	Negative
CYP1A2 (pmol/ 10 ⁶ cells/min, 100 μmol L ⁻¹ Phenacetin)	68.7	81.7
OATP1B1/3 Active Estrone-3-S Uptake (pmol/ 10 ⁶ cells/min, 10 μmol L ⁻¹ Estrone-3-S) ^c	1.6	1.9
NTCP Active Taurocholate Uptake (pmol/ 10 ⁶ cells/min, 10 μmol L ⁻¹ Taurocholate) ^c	2.9	3.5

^a Body mass index (BMI) is derived from body mass (weight) divided by the square of the body height of a person.

^b Heavy Alcohol use is defined as >2 drinks per day or current history of alcoholism

^c Transporter Activity is the amount of specific substrate retained on hepatocytes after incubation with 10 μmol L⁻¹ substrates at 4°C or at 37°C for 3 min. Active uptake is the fold change between uptake at 37°C versus 4°C. The uptake is expressed in pmol per 10⁶ cells per min.

Appendix Table S3: p-Value Tables for Figures 2 to 5 in the main manuscript and Appendix Figure S3 and S5

Figure 2	Figure 2 E	AS605240 quantification								
	<i>p-value table</i>	Tissue	p-value	W						
		Lung	0,00729		0					
		Spleen	0,00729		0					
		Liver	0,2207		5					
		Kidney	0,01351		0					
		Fat	0,00729		0					
		Brain		1	10					
Figure 3	Figure 3 B	Interleukin 6 (IL-6)								
	<i>p-value table</i>	sham	PCI Vehicle	PCI T-Lipo	PCI AS					
		PCI Vehicle	2,1E-05							
		PCI T-Lipo	5,3E-05	1,0E+00						
		PCI AS	9,1E-06	1,3E-01	1,4E-01					
		PCI T-LipoAS	5,3E-05	1,4E-01	1,6E-02	2,5E-03				
	Figure 3 B	Interleukin 1 beta (IL-1β)								
	<i>p-value table</i>	sham	PCI Vehicle	PCI T-Lipo	PCI AS					
		PCI Vehicle	2,31E-02							
		PCI T-Lipo	6,16E-01	0,0231						
		PCI AS	1,07E-02	0,6162	0,0107					
		PCI T-LipoAS	7,80E-02	0,0014	0,4255	0,0014				
	Figure 3 B	Tumor Necrosis Factor alpha (TNF-α)								
	<i>p-value table</i>	sham	PCI Vehicle	PCI T-Lipo	PCI AS					
		PCI Vehicle	2,40E-05							
		PCI T-Lipo	3,70E-05	0,61407						
		PCI AS	3,40E-06	0,01025	0,03152					
		PCI T-LipoAS	4,15E-03	0,00141	0,00052	0,0001				
	Figure 3 B	Interferon gamma (IFN-γ)								
	<i>p-value table</i>	sham	PCI Vehicle	PCI T-Lipo	PCI AS					
		PCI Vehicle	0,0140							
		PCI T-Lipo	0,0000	1,0000						
		PCI AS	0,0017	0,3563	0,3563					
		PCI T-LipoAS	0,0140	1,0000	1,0000	0,3563				
	Figure 3 B	Macrophage chemotactic protein 1 (MCP-1)								
	<i>p-value table</i>	sham	PCI Vehicle	PCI T-Lipo	PCI AS					
		PCI Vehicle	1,70E-05							
	PCI T-Lipo	3,00E-05	0,58064							
	PCI AS	4,70E-06	0,0492	0,06094						
	PCI T-LipoAS	7,20E-05	0,14442	0,01105	0,00033					
Figure 3 C	Interleukin 10 (IL-10)									
<i>p-value table</i>	sham	PCI Vehicle	PCI T-Lipo	PCI AS						
	PCI Vehicle	6,96E-01								
	PCI T-Lipo	2,80E-02	0,1107							
	PCI AS	7,30E-03	0,0382	0,554						
	PCI T-LipoAS	9,39E-01	0,6858	0,0143	0,0073					
Figure 3 D	Bacterial Burden	Lavage								
<i>p-value table</i>	PCI_AS_24h	PCI_AS_48h	sham_24h	sham_48h	T-Lipo_24h	T-Lipo_48h	T-LipoAS_24h	T-LipoAS_48h	vehicle_24h	
	PCI_AS_48h	0,0227								
	sham_24h	0,0094	0,0094							
	sham_48h	0,0094	0,0094	0,4526						
	T-Lipo_24h	0,0157	0,8081	0,0190	0,2350					
	T-Lipo_48h	0,0097	0,1584	0,0190	0,2350	0,4526				
	T-LipoAS_24h	0,0094	0,6724	0,0094	0,0097	0,8081	0,3833			
	T-LipoAS_48h	0,0097	0,0808	0,0190	0,2350	0,2647	0,5464	0,1169		
	vehicle_24h	0,0175	0,1286	0,0094	0,0094	0,3360	0,8081	0,2493	0,3360	
	vehicle_48h	0,0079	0,0094	0,0094	0,0097	0,0420	0,1324	0,0175	0,6948	0,1853
Figure 3 E	Bacterial Burden	Liver								
<i>p-value table</i>	PCI_AS_24h	PCI_AS_48h	sham_24h	sham_48h	T-Lipo_24h	T-Lipo_48h	T-LipoAS_24h	T-LipoAS_48h	vehicle_24h	
	PCI_AS_48h	0,0384								
	sham_24h	0,0095	0,0095							
	sham_48h	0,0103	0,0103	0,0766						
	T-Lipo_24h	0,0521	0,9545	0,0103	0,025					
	T-Lipo_48h	0,0103	0,0459	0,0103	0,025	0,0459				
	T-LipoAS_24h	0,0208	0,6892	0,0095	0,0103	0,5012	0,025			
	T-LipoAS_48h	0,0157	0,992	0,0103	0,025	0,25	0,7526	0,1444		
	vehicle_24h	0,025	0,7724	0,0095	0,0103	0,6573	0,0727	0,9551	0,1974	
	vehicle_48h	0,0107	0,025	0,0095	0,0103	0,0992	0,5301	0,0384	0,8124	0,0414
Figure 3 F	Neutrophils	24 h								
<i>p-value table</i>	sham	PCI vehicle	PCI T-Lipo	PCI AS						
	PCI vehicle	0,36								
	PCI T-Lipo	0,36	0,77							
	PCI AS	0,77	0,53	0,36						
	PCI T-LipoAS	0,82	0,77	0,77	0,77					

Figure 3 F	Neutrophils	48 h								
	<i>p-value table</i>	sham	PCI vehicle	PCI T-Lipo	PCI AS					
	PCI vehicle	0,37								
	PCI T-Lipo	0,17	0,24							
	PCI AS	48	0,33	0,31						
PCI T-LipoAS	0,31	0,33	0,33	0,48						
Figure 3 G	Monocytes	24 h								
	<i>p-value table</i>	sham	PCI vehicle	PCI T-Lipo	PCI AS					
	PCI vehicle	0,925								
	PCI T-Lipo	0,059	0,610							
	PCI AS	0,925	0,950	0,881						
PCI T-LipoAS	0,881	0,950	0,940	1,000						
Figure 3 G	Monocytes	48 h								
	<i>p-value table</i>	sham	PCI vehicle	PCI T-Lipo	PCI AS					
	PCI vehicle	0,77								
	PCI T-Lipo	0,147	0,025							
	PCI AS	0,788	0,147	0,147						
PCI T-LipoAS	0,788	0,788	0,147	0,788						
Figure 3 H	PMN positive cells									
	<i>p-value table</i>	PCI_AS_24h	PCI_AS_48h	sham_24h	sham_48h	T-Lipo_24h	T-Lipo_48h	T-LipoAS_24h	T-LipoAS_48h	vehicle_24h
	PCI_AS_48h	0,0424								
	sham_24h	1	0,016							
	sham_48h	0,2721	0,2249	0,2249						
	T-Lipo_24h	0,0336	0,1088	0,0176	0,0722					
	T-Lipo_48h	0,0424	0,0714	0,0336	0,0536	0,9144				
	T-LipoAS_24h	0,0189	0,2278	0,0094	0,0542	0,6797	0,9144			
	T-LipoAS_48h	0,0336	1	0,009	0,2063	0,1785	0,1826	0,2249		
	sham	0,2249	0,0039	0,2249	0,0747	0,009	0,0176	0,0014	0,0014	
	Figure 4	AUC indocyanine green clearance								
<i>p-value table</i>		PCI LipoAS	PCI Vehicle	sham LipoAS						
PCI Vehicle		1,20E-06								
sham LipoAS		1,40E-05	2,40E-05							
sham Vehicle		0,11	1,40E-05	9,90E-05						
Figure 5	Survival									
	<i>p-value table</i>	PCI Vehicle	PCI AS	sham Vehicle						
	PCI AS	0,28622								
	sham Vehicle	0,00011	0,00072							
	sham AS	0,00072	0,00411	1						
Figure 5 C	Survival									
	<i>p-value table</i>	PCI Vehicle	PCI T-Lipo	PCI T-LipoAS	sham T-LipoAS					
	PCI T-Lipo	0,9135								
	PCI T-LipoAS	0,0053	0,0053							
	sham T-LipoAS	0,0028	0,003	0,0561						
sham T-Lipo	0,0103	0,0144	0,1479	1						
Appendix Figure S3	Interferon 1 beta (IFN-1β)									
	<i>p-value table</i>	sham	PCI Vehicle	PCI T-Lipo	PCI AS					
	PCI Vehicle	1,60E-03								
	PCI T-Lipo	2,89E-02	0,2542							
	PCI AS	2,89E-02	2,89E-02	0,847						
PCI T-LipoAS	7,50E-03	0,0674	0,8672	0,9049						
Appendix Figure S3	Interferon 1 beta (IFN-1β)									
	<i>p-value table</i>	sham	PCI Vehicle	PCI T-Lipo	PCI AS					
	PCI Vehicle	1,70E-02								
	PCI T-Lipo	1,99E-01	0,335							
	PCI AS	3,60E-01	0,039	0,379						
PCI T-LipoAS	3,60E-01	0,039	0,335	0,929						
Appendix Figure S3	Interleukin 1 alpha (IL-1α)									
	<i>p-value table</i>	sham	PCI Vehicle	PCI T-Lipo	PCI AS					
	PCI Vehicle	2,00E-02								
	PCI T-Lipo	1,81E-01	0,045							
	PCI AS	4,58E-01	0,055	0,807						
PCI T-LipoAS	1,00E-02	4,58E-01	0,04	0,036						
Appendix Figure S5	Survival									
	<i>p-value table</i>	PCI Vehicle	PCI Lipo	PCI LipoAS	sham Lipo					
	PCI Lipo	0,732								
	PCI LipoAS	0,1764	0,2361							
	sham Lipo	0,0014	0,0106	0,0014						
sham LipoAS	0,0888	0,1764	0,0888	1						